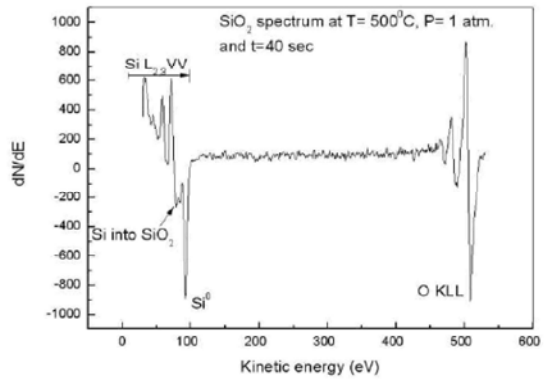

Fig. 1: Illustrative spectrum of Auger sputter depth profile of SiO_2 on Si(100)

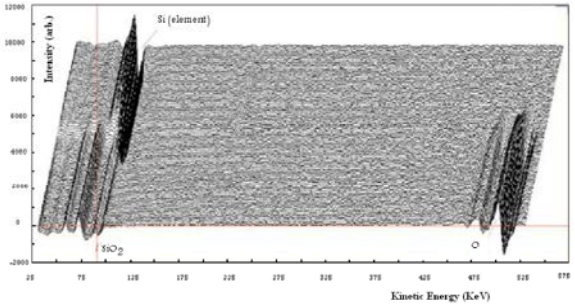

Fig. 2: Auger spectra from silicon oxide

cleans the surface, but also used to erode away the sample to reveal structure beneath the surface. In addition, the Auger electrons can escape the solid if the target atom is very near the surface. The escape depth of Auger electrons of Si (KLL) and O (KLL) are 5.5°A [1] and 5-15°A [2] independently on energy of the incident electron beam, i.e. Auger electrons are only emitted from the outermost atomic layers. Hence, the energy of these electrons is counted and resulted an spectrum of number of electrons of the Auger peaks to identify the elements present in the sample, as it was found before [3-8] (Figures 1, 2).

Figure 1 shows an Auger sputter depth profile of SiO_2 on Si(100). Auger measurements were alternated with sputtering and the sputter time varies along the direction of the plots. The sample was sputtered for 30 seconds between measurements. Additional information is available in published literature from the author's recent work [4-6]. In addition, Figure 2 illustrates the SiO_2 spectrum peaks at 62 and 78 eV; the Si, O peaks are due to reduction of SiO_2 by the electron beam.

The Auger process is quite remarkable by the tremendous range of energy over which this phenomenon is observed. Using the first order derivative of the signal it is possible to get a better line assignment, because of the maximum peak at special energy where the elements present, generates a resonance like structure in $dN(E) / d(E)$, whose most negative excursion at this energy corresponds to the steepest slope of the N(E).

DISCUSSION

The characteristic Auger spectra from silicon oxide and silicon are shown in Figures 2 and 3. The signal from each element has a characteristic shape and is determined using reference and moreover, Plasmon peaks can be distinguished from Auger peaks by their layer width as well. As shown in these figures, the typical sharp of minima of Si and O at 92 eV and 510 eV, respectively. These peaks followed by series of smaller peaks, the latter being due partly to other Auger components. The 92 eV peak is due to elemental silicon, but most of the following two peaks are due to silicon in silicon oxide. In fact, a steam oxidized sample produced only the last two peaks and no 92 eV peak. However, electron beam bombardment caused sufficient decomposition to produce some elemental silicon.

Figure 2 depicts the sputtering spectrum silicon with using 5 keV energy of Ar ion (Ar^+). It would help one to get further information about the specimen. Indeed, one is able to drill a hole in the specimen at some specified spot and clean the surface as well. For this purpose one can plot the signal strengths of selected Auger transition as a function of the sputtering time (Figures 3, 4 and 5). It is so important to choose the size of the Ar^+ beam spot for rastering a crater with a flat boom surface. The small-spot focused-beam provides a good solution for a wide range of applications. As one can see in these figures (Figures 1 and 2), the Si into SiO_2, Auger signal decreases considerably at near interface and then the Plasmon peak at 75 eV increase to a high value corresponds to the Si substrate. More detail information reported in the literature [9-15].

Although departure from linear-parabolic kinetics [16] in the functional dependence, however, is the same over a large parameter range. An initial linear dependence with respect to time; follows by an extensive parabolic regime. It means that evolution of concentration is time-dependence and so the gradient of oxidant species is not constant. The enhanced initial oxidation rate (Figure 3) has been described earlier [17-19] as an exponentially decaying extra rate them, together with detailed extraction of relevant activation energies.

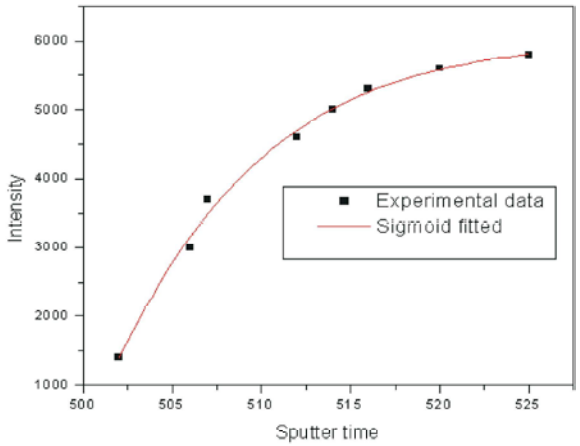

Fig. 3: The oxygen Intensity versus the sputer time.

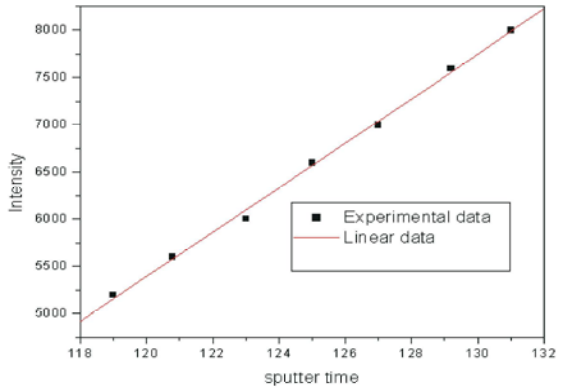

Fig. 4: The silicon intensity versus the sputter time

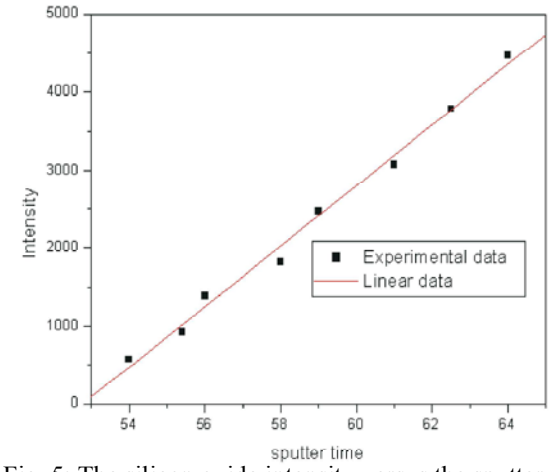

Fig. 5: The silicon oxide intensity versus the sputter time.

CONCLUSION

The vital role of very thin dielectrics is well defined in nano-electric field. The necessary attempt and motivation for characterization of silicon oxide in the thin regimes preformed. In the dry thermal oxidation process with Si the growth rate of the initial parts of the reaction is currently modeled with additional terms, besides the usual linear-parabolic time dependency. It was great achievement to find the similar oxide growth as Deal-Grove / Massoud predicted, but it is as limiting case emerging from the Boltzmann-like expression.

REFERENCES

1. Bahari, A., U. Robenhagen, P. Morgen and Z. Li, 2005. Growth of ultrathin silicon nitride on Si (111) at low temperature, Physical Review B, Vol. 72, No. 20: 205323-9. Doi/10.1103/PhysRevB.72.205323
2. Bahari, A., P. Morgen and Z.S. Li, 2006. Valence band studies of the formation of ultrathin pure silicon nitride film on Si(100), Surface science, Vol. 600, No. 15: 2966-2971.
3. Bahari, A., P. Morgen, K. Pederson and Z. Li, 2006. Growth of a stacked silicon nitride / silicon oxide dielectric on Si(100). Journal of Vacuum Science & Technology B: Microelectronics and Nanometer Structures, 24(4): 242119-2123.
4. Bahari, A., P. Morgen and Z.S. Li, 2008. Ultra thin silicon nitride films on Si (100) studied with core level photoemission. Surface Science, 602(13): 2315-2324.
5. Hernandez-Torres, J. and A. Mendoza-Galvan, 2005. Formation of NiO-SiO_2 nanocomposite thin films by the sol gel method. Journal of non-crystalline Solids, 351(24): 2029-2035.
6. Wilk, G.D., R.M. Wallace and J. Anthony, 2001. High-k gate dielectrics: Current status and materials properties considerations. Journal of Applied Physics, 89(10): 5243-5275.
7. Arden, M.W., 2002. The International Technology Roadmap for Semiconductors, Perspectives and challenges for the next 15 years. Current Opinion in Solid State and Materials Science, 6(5): 371-377.
8. Nohira, H., *et al.* 2004. Atomic-scale depth profiling of composition, chemical structure and electronic band structure of La2O3/Si (100) interfacial transition layer. Applied Surface Science, 234(1): 493-496.
9. Ng, J.A., N. Sugii, K. Kakushima, P. Ahmet, K. Tsutsui, T. Hattori and H. Iwai, 2006. Effective mobility and interface-state density of La2O3 nMISFETs after post deposition annealing. IEICE Electronics Express, 3(13): 316-321.
10. Toriumi, A., *et al.* 2005. Advantages of HfAlON gate dielectric film for advanced low power CMOS application. Microelectronic Engineering, 80: 190-197.

11. Chin, A., Y. Wu, S. Chen, C. Liao and W. Chen, 2000. High quality La_2O_3 and Al_2O_3 gate dielectrics with equivalent oxide thickness 5-10 Ã…. in VLSI Technology, 2000. Digest of Technical Papers. 2000 Symposium on. 2000: IEEE.
12. Ng, J., Y. Kuroki, N. Sugii, K. Kakushima, S.I. Ohmi, K. Tsutsui, T. Hattori, H. Iwai and H. Wong, 2005. Effects of low temperature annealing on the ultrathin La_2O_3 gate dielectric; comparison of post deposition annealing and post metallization annealing. Microelectronic Engineering, 80: 206-209.
13. Bertoluzza, A., C. Fagnano, M. Antonietta Morelli, V. Gottardi and M. Guglielmi, 1982. Raman and infrared spectra on silica gel evolving toward glass. Journal of Non-crystalline Solids, 48(1): 117-128.
14. Song, Y., S. Dhar, L. Feldman, G. Chung and J. Williams, 2004. Modified Deal Grove model for the thermal oxidation of silicon carbide. Journal of Applied Physics, 95(9): 4953-4957.
15. Deal, B.E. and A. Grove, 1965. General relationship for the thermal oxidation of silicon. Journal of Applied Physics, 36(12): 3770-3778.
16. Massoud, H., 1997. Thermal oxidation of silicon in the ultrathin regime. Solid-State Electronics, 41(7): 929-934.
17. Lewis, E. and E. Irene, 1987. The effect of surface orientation on silicon oxidation kinetics. Journal of The Electrochemical Society, 134(9): 2332-2339.
18. Chabal, Y.J., Fundamental aspects of silicon oxidation. Vol. 46. 2001: Springer Verlag.